

Measurements of Higgs boson production by gluon-gluon fusion and vector-boson fusion using $H \rightarrow WW^* \rightarrow e\nu\mu\nu$ decays in pp collisions at $\sqrt{s} = 13$ TeV with the ATLAS detector

Phys. Rev. D 108 (2023) 032005

Badr-eddine Ngair (obo the group **B**)

ASIA EUROPE PACIFIC SCHOOL OF HIGH-ENERGY PHYSICS-2024

23-June-2024



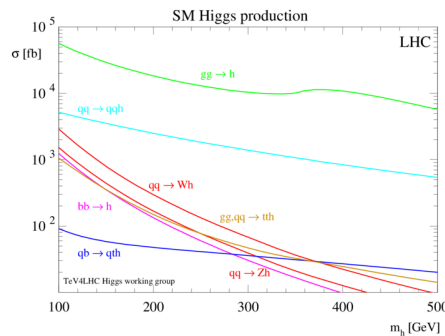
1 Introduction

2 Measurements of Higgs boson production

3 Results

Motivation

Measurements of the Higgs **properties** are a powerful test of the **SM** and can be used to constrain theories of physics beyond the SM (**BSM**).



Introduction

- 1 Measurement of Higgs boson production by gluon-gluon fusion (**ggF**) and vector-boson fusion (**VBF**)

- 2 The decay $H \rightarrow WW^* \rightarrow e\nu\mu\nu$

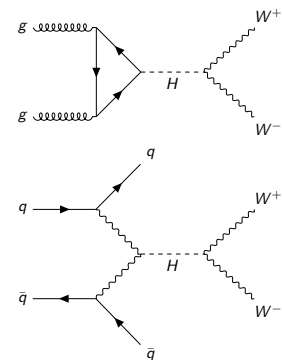
- Large branching ratio
- Low-level backgrounds: different flavor of charged leptons in final state

- 3 Previous measurements

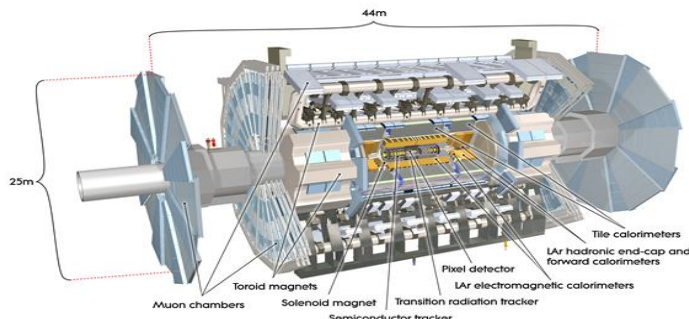
- ATLAS [[PLB 789 \(2019\) 508](#)], $\sqrt{s} = 13 \text{ TeV}$, $\mathcal{L} = 36 \text{ fb}^{-1}$
- CMS [[JHEP 03 \(2021\) 003](#)] $\sqrt{s} = 13 \text{ TeV}$, $\mathcal{L} = 137 \text{ fb}^{-1}$

- 4 Additions for full **Run 2** Analysis (relative to the 36 fb^{-1} Analysis)

- Include of ggF **Njets ≥ 2** region
- VBF signal tagging with a **ML** technique (DNN).
- **Simplified Template Cross Section** (STXS) stage 1.2



ATLAS Detector



- ① Data taken from pp collision at $\sqrt{s} = 13$ TeV, using the full Run2 dataset with $\mathcal{L} = 139 \text{ fb}^{-1}$
- ② MC simulation for signal and backgrounds generated via standard generators like POWHEG, Pythia, MadGraph and Sherpa

1 Introduction

2 Measurements of Higgs boson production

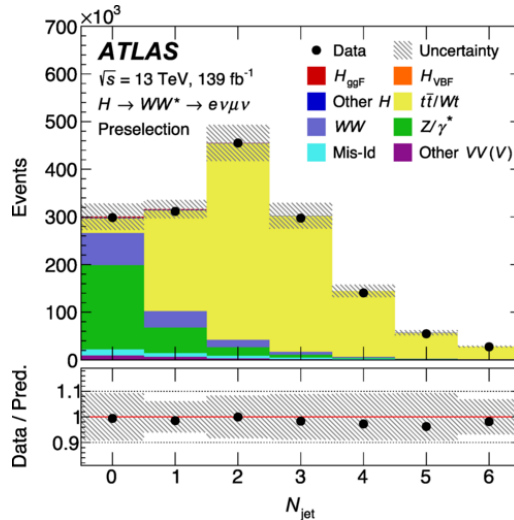
3 Results

Event Reconstruction

- ① Tracks $p_T > 500$ MeV
- ② \geq one primary vertex with \geq two associated tracks
- ③ Electrons
 - Excluding the transition region between the barrel and end caps of the LAr calorimeter
- ④ Muons
 - Inner tracker and muon spectrometer
- ⑤ Trigger objects must be matched to at least one of offline reconstructed leptons

Event Selection

- Two isolated leptons with opposite charge and different flavour $\alpha = (e, \mu)$
- $p_T(l_1) > 22$ GeV
- $p_T(l_2) > 15$ GeV
- $\tau\tau$ Background reduction
 - $m_{ll} > 10$ GeV
 - $p_T^{\text{miss}} > 20$ GeV (only ggF)



Event Categorization

$N_j=0$

- Sensitive to ggF
- discriminant for bkg: $\Delta\phi_{\ell\ell} < 0.8$ and $\Delta m_{\ell\ell} < 55$ GeV

$N_j=1$

- Sensitive to ggF
 - discriminant for the bkg: $\max(m_T^{\ell_i}) > 50$ GeV
- $$m_T^{\ell_i} = \sqrt{2p_T^{\ell_i} E_T^{\text{miss}} (1 - \cos\Delta\phi(\ell_i, E_T^{\text{miss}}))}$$

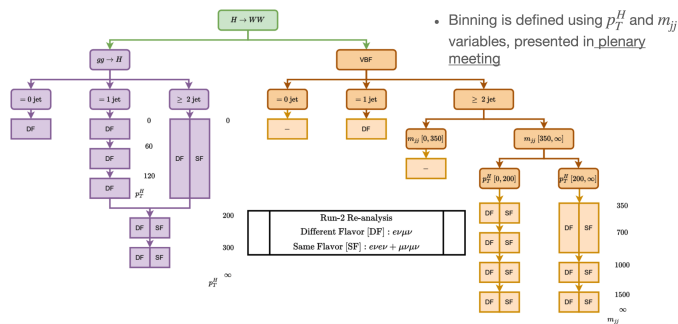
$N_j \geq 2$

- Sensitive to ggF and VBF
- For ggF : $|m_{jj}-85| < 15$ GeV, $\Delta y_{jj} < 1.2$, $\Delta\phi_{\ell\ell} < 0.8$ and $\Delta m_{\ell\ell} < 55$ GeV
- For VBF: Deep Neural Network (DNN) trained on 15 variables

→ Dominant bkg includes $WW, t\bar{t}/Wt, Z/\gamma^*$ in above categories

STXS (Stage 1.2)

Simplified template cross sections (STXS) are an approach to categorise the Higgs-boson candidate events according to the properties associated with the Higgs production mode. This allows physicists to characterise the Higgs boson independently of its decay channel.



Systematic uncertainties

| Source | $\frac{\Delta\sigma_{\text{ggF+VBF}} \cdot B_{H \rightarrow WW^*}}{\sigma_{\text{ggF+VBF}} \cdot B_{H \rightarrow WW^*}} [\%]$ | $\frac{\Delta\sigma_{\text{ggF}} \cdot B_{H \rightarrow WW^*}}{\sigma_{\text{ggF}} \cdot B_{H \rightarrow WW^*}} [\%]$ | $\frac{\Delta\sigma_{\text{VBF}} \cdot B_{H \rightarrow WW^*}}{\sigma_{\text{VBF}} \cdot B_{H \rightarrow WW^*}} [\%]$ |
|--------------------------------|--|--|--|
| Data stat uncertainties | 4.6 | 5.1 | 15 |
| Total sys uncertainties | 9.5 | 11 | 18 |
| Total | 10 | 12 | 23 |

ggF signal: measurement of exclusive jet multiplicities

VBF signal: different generators for the matrix-element matching

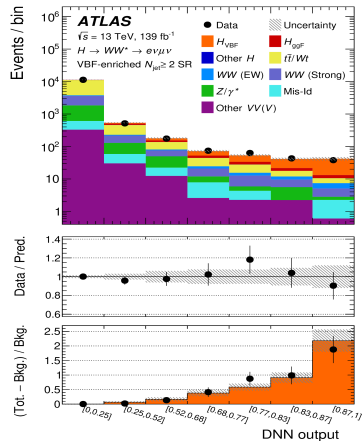
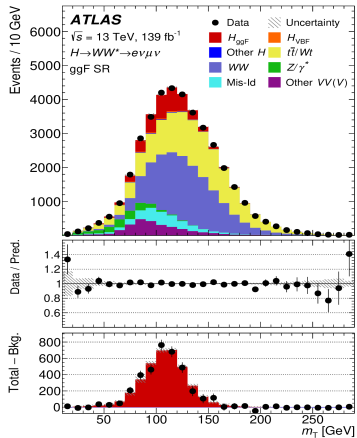
Background: theoretical uncertainties in the WW and top-quark

1 Introduction

2 Measurements of Higgs boson production

3 Results

Post-fit m_T and DNN distributions



Post-fit SR yields

| Process | $N_{\text{jet}} = 0$ ggF | $N_{\text{jet}} = 1$ ggF | $N_{\text{jet}} \geq 2$ ggF | $N_{\text{jet}} \geq 2$ VBF | |
|------------------|--------------------------|--------------------------|-------------------------------|-----------------------------|-----------------|
| | | | DNN: Inclusive [0.87, 1.0] | | |
| H_{ggF} | 2100 ± 220 | 1100 ± 130 | 440 ± 90 | 209 ± 40 | 2.6 ± 0.9 |
| H_{VBF} | 23 ± 9 | 103 ± 30 | 46 ± 12 | 180 ± 40 | 28.8 ± 5.5 |
| Other Higgs | 40 ± 20 | 55 ± 28 | 55 ± 27 | 29 ± 15 | 0.04 ± 0.02 |
| WW | 9700 ± 350 | 3500 ± 410 | 1500 ± 470 | 2100 ± 340 | 4.6 ± 1.2 |
| $t\bar{t}/Wt$ | 2200 ± 210 | 5300 ± 340 | 6100 ± 500 | 7600 ± 370 | 2.6 ± 0.8 |
| Z/γ^* | 140 ± 50 | 280 ± 40 | 930 ± 70 | 1300 ± 300 | 0.6 ± 0.1 |
| Other VV | 1400 ± 130 | 840 ± 100 | 470 ± 90 | 380 ± 80 | 0.6 ± 0.1 |
| Mis-Id | 1200 ± 130 | 720 ± 90 | 470 ± 50 | 330 ± 40 | 1.7 ± 0.2 |
| Total | $16\,770 \pm 130$ | $11\,940 \pm 110$ | $10\,030 \pm 100$ | $12\,200 \pm 180$ | 42.0 ± 5.1 |
| Observed | 16 726 | 11 917 | 9 982 | 12 189 | 38 |

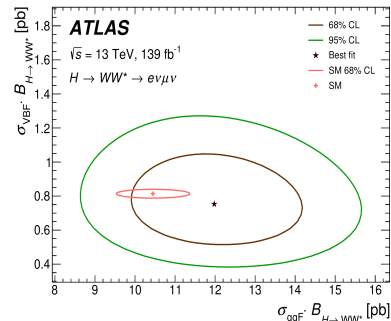
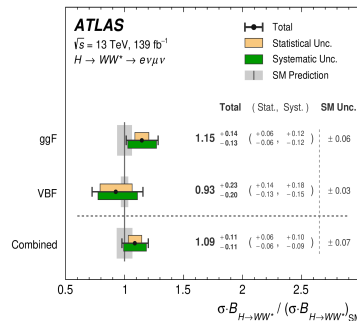
Inclusive cross-section

$$\sigma_{\text{ggF}} \cdot \mathcal{B}_{H \rightarrow WW^*} = 12.0 \pm 1.4 \text{ pb}$$

$$(\sigma_{\text{ggF}} \cdot \mathcal{B}_{H \rightarrow WW^*})^{\text{SM}} = 10.4 \pm 0.5 \text{ pb}$$

$$\sigma_{\text{VBF}} \cdot \mathcal{B}_{H \rightarrow WW^*} = 0.75^{+0.19}_{-0.16} \text{ pb}$$

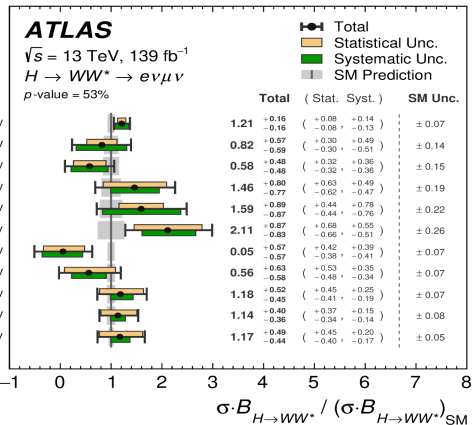
$$(\sigma_{\text{VBF}} \cdot \mathcal{B}_{H \rightarrow WW^*})^{\text{SM}} = 0.81 \pm 0.02 \text{ pb}$$



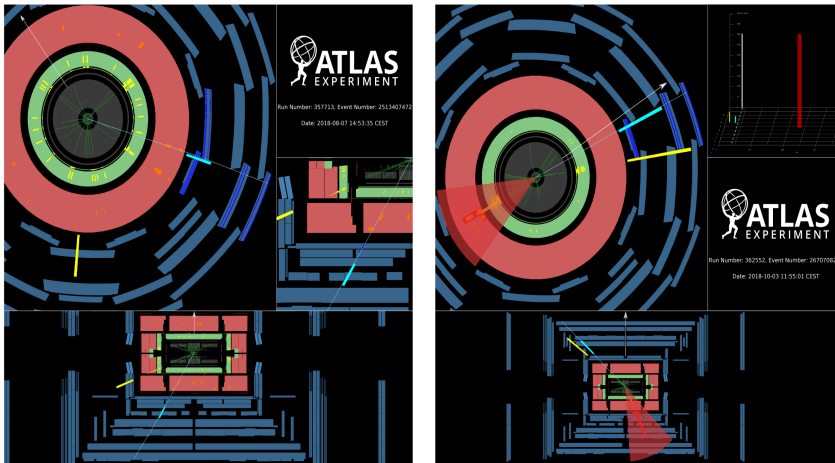
$$\sigma_{\text{ggF} + \text{VBF}} \cdot \mathcal{B}_{H \rightarrow WW^*} = 12.3 \pm 1.3 \text{ pb}$$

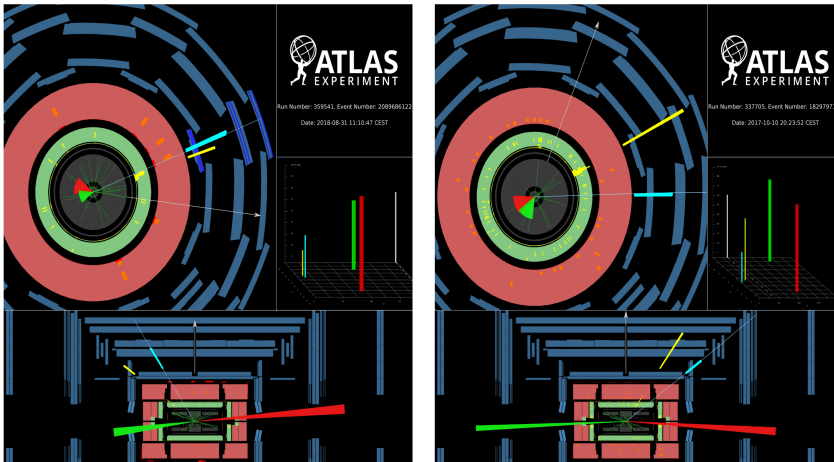
$$(\sigma_{\text{ggF} + \text{VBF}} \cdot \mathcal{B}_{H \rightarrow WW^*})^{\text{SM}} = 11.3 \pm 0.5 \text{ pb}$$

STXS results



- The analysis is extended to include measurements of production cross-sections in **11 kinematic fiducial regions** (STXS) for the first time in this decay channel.
- Agreement with the SM with a p-value of **53%**

Event display - ggF $N_j = 0$ (left) and 1 (right)

Event display - ggF $N_j \geq 2$ (left) and VBF (right)

Summary

- ① This paper constitutes the first full Run 2 cross section measurements of ggF+VBF $H \rightarrow WW^*$ in ATLAS
- ② $H \rightarrow WW^*$ cross section measured in each of the STXS bins, normalized to the corresponding SM prediction are done.
- ③ Looking forward to use run3 data and combine run2+run3.

Thank you for your attention!

Back-Up

Systematic uncertainties (2)

Experimental uncertainties

- ① Uncertainties arise from the jet energy scale (JES) and resolution (JER), JVT, and the jet ID
- ② Uncertainties due to the trigger selection
- ③ Uncertainties for the soft term in the reconstruction od MET
- ④ combined 2015–2018 integrated luminosity is 1.7%
- ⑤ Uncertainty in the modeling of pileup
- ⑥ uncertainty on the electron (muon) ranging from 10% (12%) at low pt to 35% (75%) at high pt.

Theoretical uncertainties

- ① For signal, top, and Z/Γ
 - parton shower and the matrix-element
- ② qqWW and of WZ, ZZ and $V\gamma^*$
 - variations of the matching scale and nonperturbative effects
- ③ For signal processes
 - variations of the matching scale and nonperturbative effects
 - factorization and renormalization scales.
- ④ The ggWW process:
 - conservative 50%/+100% normalization uncertainty

Simulation tools

| Process | Matrix element | PDF set | UEPS model | Prediction for total cross section |
|------------------------------------|--|---------------|------------------------|------------------------------------|
| ggF H | Powheg Box v2 NNLOPS (MG5_aMC@NLO) | PDF4LHC15nnlo | Pythia 8 (Herwig 7) | N3LO QCD + NLO EW |
| VBF H | Powheg Box v2 (MG5_aMC@NLO) | PDF4LHC15nlo | Pythia 8 (Herwig 7) | NNLO QCD + NLO EW |
| VH excluding $gg \rightarrow ZH$ | Powheg Box v2 | PDF4LHC15nlo | Pythia 8 | NNLO QCD + NLO EW |
| $t\bar{t}H$ | Powheg Box v2 | NNPDF3.0nlo | Pythia 8 | NLO |
| $gg \rightarrow ZH$ | Powheg Box v2 | PDF4LHC15nlo | Pythia 8 | NNLO QCD + NLO EW |
| $qq \rightarrow WW$ | Sherpa 2.2.2 | NNPDF3.0nnlo | Sherpa 2.2.2 | NLO |
| $qq \rightarrow WWqq$ | MG5_aMC@NLO | NNPDF3.0nlo | Pythia 8 (Herwig 7) | LO |
| $gg \rightarrow WW/ZZ$ | Sherpa 2.2.2 | NNPDF3.0nnlo | Sherpa 2.2.2 | NLO |
| $WZ/V\gamma^*/ZZ$ | Sherpa 2.2.2 | NNPDF3.0nnlo | Sherpa 2.2.2 | NLO |
| $V\gamma$ | Sherpa 2.2.8 | NNPDF3.0nnlo | Sherpa 2.2.8 | NLO |
| VVV | Sherpa 2.2.2 | NNPDF3.0nnlo | Sherpa 2.2.2 | NLO |
| $t\bar{t}$ | Powheg Box v2 (MG5_aMC@NLO) | NNPDF3.0nlo | Pythia 8 (Herwig 7) | NNLO+NNLL |
| Wt | Powheg Box v2 (MG5_aMC@NLO) | NNPDF3.0nlo | Pythia 8 (Herwig 7) | NNLO |
| Z/γ^* | Sherpa 2.2.1 (MG5_aMC@NLO) | NNPDF3.0nnlo | Sherpa 2.2.1 | NNLO |

Systematic uncertainties

Uncertainties from both experimental and theoretical sources affect the results of the analysis

| Source | $\frac{\Delta \sigma_{ggF+VBF} \cdot B_{H \rightarrow WW^*}}{\sigma_{ggF+VBF} \cdot B_{H \rightarrow WW^*}}$ [%] | $\frac{\Delta \sigma_{ggF} \cdot B_{H \rightarrow WW^*}}{\sigma_{ggF} \cdot B_{H \rightarrow WW^*}}$ [%] | $\frac{\Delta \sigma_{VBF} \cdot B_{H \rightarrow WW^*}}{\sigma_{VBF} \cdot B_{H \rightarrow WW^*}}$ [%] |
|--------------------------------|--|--|--|
| Data statistical uncertainties | 4.6 | 5.1 | 15 |
| Total systematic uncertainties | 9.5 | 11 | 18 |
| MC statistical uncertainties | 3.0 | 3.8 | 4.9 |
| Experimental uncertainties | 5.2 | 6.3 | 6.7 |
| Flavor tagging | 2.3 | 2.7 | 1.0 |
| Jet energy scale | 0.9 | 1.1 | 3.7 |
| Jet energy resolution | 2.0 | 2.4 | 2.1 |
| $E_{\text{miss}} T$ | 0.7 | 2.2 | 4.9 |
| Muons | 1.8 | 2.1 | 0.8 |
| Electrons | 1.3 | 1.6 | 0.4 |
| Mis-Id extrapolation factors | 2.1 | 2.4 | 0.8 |
| Pileup | 2.4 | 2.5 | 1.3 |
| Luminosity | 2.1 | 2.0 | 2.2 |
| Theoretical uncertainties | 6.8 | 7.8 | 16 |
| ggF | 3.8 | 4.3 | 4.6 |
| VBF | 3.2 | 0.7 | 12 |
| WW | 3.5 | 4.2 | 5.5 |
| Top | 2.9 | 3.8 | 6.4 |
| $Z\tau\tau$ | 1.8 | 2.3 | 1.0 |
| Other VV | 2.3 | 2.9 | 1.5 |
| Other Higgs | 0.9 | 0.4 | 0.4 |
| Background normalizations | 3.6 | 4.5 | 4.9 |
| WW | 2.2 | 2.8 | 0.6 |
| Top | 1.9 | 2.3 | 3.4 |
| $Z\tau\tau$ | 2.7 | 3.1 | 3.4 |
| Total | 10 | 12 | 23 |

Event selection and categorization

| Category | $N_{\text{jet},(p_T>30 \text{ GeV})} = 0 \text{ ggF}$ | $N_{\text{jet},(p_T>30 \text{ GeV})} = 1 \text{ ggF}$ | $N_{\text{jet},(p_T>30 \text{ GeV})} \geq 2 \text{ ggF}$ | $N_{\text{jet},(p_T>30 \text{ GeV})} \geq 2 \text{ VBF}$ |
|---|--|---|--|--|
| Preselection | Two isolated, different-flavor leptons ($\ell = e, \mu$) with opposite charge $p_T^{\text{lead}} > 22 \text{ GeV}$, $p_T^{\text{sublead}} > 15 \text{ GeV}$ $m_{\ell\ell} > 10 \text{ GeV}$ $p_T^{\text{miss}} > 20 \text{ GeV}$ | | | |
| | $N_{b\text{-jet},(p_T>20 \text{ GeV})} = 0$ $\Delta\phi_{\ell\ell, E_T^{\text{miss}}} > \pi/2$ $p_T^{\ell\ell} > 30 \text{ GeV}$ | | | |
| Background rejection | $m_{\tau\tau} < m_Z - 25 \text{ GeV}$ $\max(m_T^\ell) > 50 \text{ GeV}$ | | | |
| | $m_{\ell\ell} < 55 \text{ GeV}$ $\Delta\phi_{\ell\ell} < 1.8$ | | | |
| $H \rightarrow WW^* \rightarrow e\nu\mu\nu$ topology | | | fail central jet veto or fail outside lepton veto $ m_{jj} - 85 > 15 \text{ GeV}$ or $\Delta y_{jj} > 1.2$ | |
| | | | central jet veto outside lepton veto $m_{jj} > 120 \text{ GeV}$ | |
| Discriminating fit variable | m_T | | | DNN |

Analysis Overview

① Event Characterization

- two leptons + two neutrinos (MET)

② Background composition varies with jet count Njet.

- ggF: Njet = 0, 1, and ≥ 2 (targeted by Dilepton Transverse Mass m_T)

$$m_T = \sqrt{(E_{\ell\ell} + E_T^{\text{miss}})^2 - |\mathbf{p}_{T,\ell\ell} + \mathbf{E}_T^{\text{miss}}|^2}$$

- VBF: Njet ≥ 2 (targeted by a Deep Neural Network (DNN) trained on 15 variables using lepton, jet and E_T^{miss} information)

③ STXS framework is conducted to measure the cross-section

- ggF: higher-order QCD and EW corrections
- VBF: ($V \rightarrow q\bar{q}$)H topology